Journal of Solid State Chemistry **155,** 250–258 (2000)
doi:10.1006/jssc.2000.8961, available online at http://www.idealibrary.com on IDEAL®

Single Crystal Structural Investigations on $Ni_yMo_6Se_{8-x}S_x$ Solid Solution: A New Location of Nickel Counterions

S. Belin,[1] R. Chevrel,[2] and M. Sergent

Laboratoire de Chimie du Solide et Inorganique Moléculaire (LCSIM), UMR CNRS 6511, Campus de Beaulieu, Université de Rennes1, 35042 Rennes Cedex, France

Received May 16, 2000; in revised form September 5, 2000; accepted September 6, 2000

DEDICATED TO PROFESSOR J. M. HONIG

The structures of nickel sulfoselenide Chevrel phases have been determined. All the richest nickel phases crystallize in rhombohedral symmetry. A single-crystal structural study makes it possible to identify the special nickel cation locations inside the host network for both pure sulfide and selenide Chevrel phases. We also show that these nickel atoms can form some kind of cluster in the cavities of the host or Ni–Mo bondings.

Key Words: **Chevrel phases; chalcogen solid solution; crystal structural determination; Ni–Ni and Ni–Mo bondings.**

I. INTRODUCTION

The ternary molybdenum chalcogenides $M_yMo_6X_8$ (M = metal ion and X = S, Se, or Te), the so-called Chevrel phases, have been extensively studied for their unusual properties, such as superconductivity and magnetic and thermoelectric behavior (1–3), because of their interesting structure.

The Chevrel phases structure is based on pseudo-molecular quasi-rigid Mo_6X_8 units, with three-dimensional secant channels between units where are located in vacant sites that can accommodate M^{n+} cations. The nature and number of cations control the symmetry of these phases.

This family of compounds contains complete solid solutions when sulfur atoms substitute to selenium atoms. The first solid solution studied was $Pb_yMo_6Se_{8-x}S_x$ (4) in 1975. Chevrel *et al.*, showed the correlations between T_c (superconducting critical temperature) and structural parameters such as the rhombohedral angle α_R. Later, Tarascon reported several series $M_yMo_6Se_{8-x}S_x$ (M = Cu, Ag, Pb, Yb, Eu, Sr, La) and was interested in chalcogen ordering in the host network according to cation content (5).

We focused our interest on $Ni_yMo_6Se_{8-x}S_x$, nickel chalcogenide solid solutions, because Chevrel phase series containing small cations, have been much less studied, but they have recently exhibited interesting physical properties (3). $Ni_yMo_6Se_{8-x}S_x$ presents some unexplained differences with other Chevrel phases containing small cations. For instance, the whole $Cu_yMo_6Se_{8-x}S_x$ ($0 \le y \le 4$ and $x \le 8$) solid solution crystallizes in the rhombohedral–hexagonal system at room temperature (6, 7), while $Ni_yMo_6Se_{8-x}S_x$ is more complex. Indeed in this solid solution, nickel Chevrel selenides can crystallize at room temperature in rhombohedral or triclinic structure according to the y amount of nickel element (8). On the one hand, the only known structure in the system Ni–Mo–Se was one of $Ni_{0.66}Mo_6Se_8$ with triclinic symmetry (9), equivalent to triclinic nickel telluride compound $Ni_{0.85}Mo_6Se_8$ (10). The nickel y solid solution in $Ni_yMo_6Se_8$ exhibited compounds with rhombohedral symmetry at higher y Ni content (8). On the other hand, the pure nickel molybdenum sulfides $Ni_yMo_6S_8$ crystallize in rhombohedral symmetry with the structure like to $Cu_yMo_6(S, Se)_8$ (6, 7). Pure nickel molybdenum sulfide and selenide present very large differences in the location of the nickel cations. So we expected to explain such differences in sulfoselenide Chevrel phases with small cations by studying accurately the crystallographic structure of this chalcogen solid solution.

We expected also to increase our knowledge of the symmetry of the Chevrel phases in relation to inserted cations.

The atomic positions determination is also important for band structure calculations (3). We report the synthesis and powdered X-ray diffraction results of $Ni_{1.2}Mo_6Se_{8-x}S_x$ compounds. We also investigate the richest nickel solid solution to follow the location of the Ni atoms in the chalcogen network by single crystal structural investigations.

II. EXPERIMENTAL

Phases of composition $Ni_{1.2}Mo_6Se_{8-x}S_x$ (with a step x of 0.5) were prepared by reaction of stoichiometric mixtures of

[1] Current address: Laboratoire pour l'Utilisation du Rayonnement Synchrotron (LURE), Université Paris-Sud, 91405 Orsay, France.

[2] To whom correspondence should be addressed. Tel.: 00 33 2 99 28 62 51; Fax: 00 33 2 99 63 57 04; E-mail:chevrel@univ-rennes1.fr.

0022-4596/00 $35.00

MoS_2 and $MoSe_2$ binary powders and Mo and Ni metallic powders pressed into a pellet and then sealed in evacuated quartz tube. After being heated around 1200°C for one week, the samples were quenched in water (to prevent $MoSe_{2-z}S_z$ ($0 \leq z \leq 2$) from forming).

Single crystals were made in the same way, but the y amount of nickel was fixed to 2, so the extra nickel with chalcogen atoms can act as transport agent and the y amount of nickel be maximum (y_{max}). The time of crystallization was extended for one week more and the compounds were slowly cooled according to the inertia of the furnace.

III. RESULTS AND DISCUSSION

III.1. $Ni_{1.2}Mo_6Se_{8-x}S_x$ Series

The X-ray data of the pseudo-ternary chalcogen system $Ni_{1.2}Mo_6Se_{8-x}S_x$ indicate that the samples have rhombohedral symmetry ($R\bar{3}$) over the whole range of composition $0 \leq x < 8$. Note that $Ni_{1.2}Mo_6S_8$ is a metastable compound only obtained by low-temperature diffusion of Ni element in α-Mo_6S_8 host compound (11).

Figures 1 and 2 show respectively the hexagonal unit-cell parameters a_H and c_H and the hexagonal volume V_H versus x, the sulfur amount. The a_H and c_H parameters decrease quasi-monotonically as x increases, and the hexagonal volume shows a slightly negative deviation from Vegard's law.

On Fig. 3, we consider the variation of the ratio c_H/a_H or the rhombohedral angle α_R as function of x. Near the value $x = 3.5$–4, the curves present an inflexion point. We observe a "quasi-plateau" around these values.

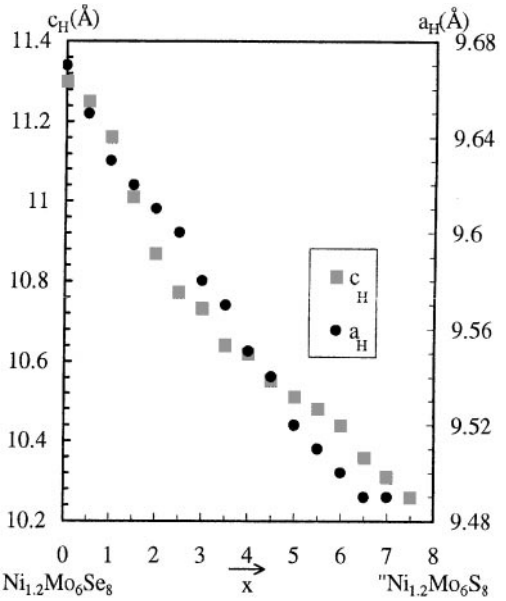

FIG. 1. Variation of a_H and c_H hexagonal unit-cell parameters as function of x sulfur content in $Ni_{1.2}Mo_6Se_{8-x}S_x$.

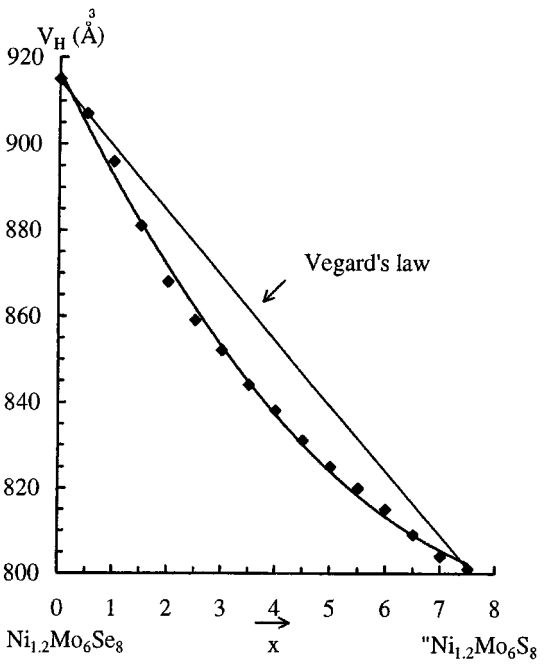

FIG. 2. Hexagonal unit-cell volume of $Ni_{1.2}Mo_6Se_{8-x}S_x$ crystalline powders.

Two assumptions can explain such a feature: a modification of chalcogen disorder or a change of sites filled by the Nickel cations.

III.2. $Ni_yMo_6Se_{8-x}S_x$ ($y \sim 2$) Single Crystals

The crystal growth has been carried out as it is described previously. We have investigated five single crystals with

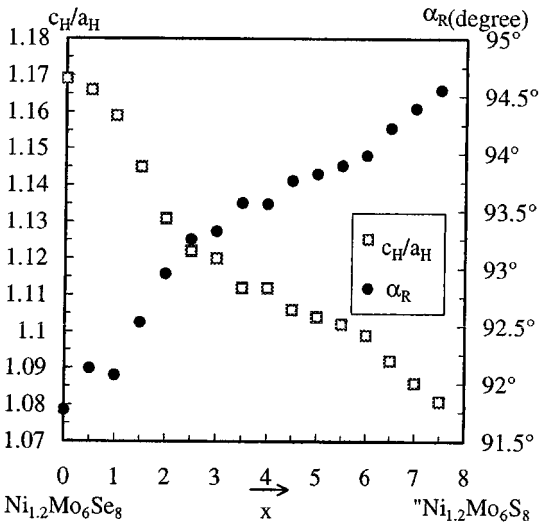

FIG. 3. Variation of the c_H/a_H hexagonal unit-cell parameters ratio and the rhombohedral angle α_R versus the sulfur content x of $Ni_{1.2}Mo_6Se_{8-x}S_x$ solid solution.

TABLE 1
Crystal Data and Experimental Parameters for the Intensity Data Collection of $Ni_{1.25}Mo_6Se_8$, $Ni_{1.28}Mo_6Se_{5.72}S_{2.28}$, $Ni_{1.82}Mo_6Se_{4.11}Se_{3.89}$, $Ni_{1.85}Mo_6Se_{3.46}S_{4.54}$, $Ni_{1.99}Mo_6Se_{2.17}S_{5.83}$

I. Crystal Data

Formula:	$Ni_{1.25}Mo_6Se_8$,		M: 1280.71 g/mol
	$Ni_{1.28}Mo_6Se_{5.72}S_{2.28}$,		M: 1218 g/mol
	$Ni_{1.82}Mo_6Se_{4.11}S_{3.89}$		M: 1314 g/mol
	$Ni_{1.85}Mo_6Se_{3.46}S_{4.54}$		M: 1103 g/mol
	$Ni_{1.99}Mo_6Se_{2.17}S_{5.83}$		M: 1050.75 g/mol
Crystal system:	rhombohedral	space group:	R-3 (No. 148)
Parameters:	$a_R = 6.7316$ (9) Å	$\alpha_r = 91.183°$ (2)	$V_r = 304.60$ (2) Å^3
	$a_R = 6.6313$ (3) Å	$\alpha_r = 93.106°$ (6)	$V_r = 290.27$ (5) Å^3
	$a_R = 6.5790$ (3) Å	$\alpha_r = 93.875°$ (7)	$V_r = 282.71$ (5) Å^3
	$a_R = 6.5628$ (3) Å	$\alpha_r = 94.055°$ (5)	$V_r = 280.43$ (4) Å^3
	$a_R = 6.5079$ (6) Å	$\alpha_r = 94.37°$ (1)	$V_r = 273.09$ (9) Å^3
	$a_H = 9.670$ (2) Å	$c_H = 11.282$ (5) Å	$V_H = 913.7$ (4) Å^3
	$a_H = 9.629$ (1) Å	$c_H = 10.845$ (8) Å	$V_H = 870.8$ (1) Å^3
	$a_H = 9.613$ (1) Å	$c_H = 10.597$ (1) Å	$V_H = 848.1$ (1) Å^3
	$a_H = 9.604$ (1) Å	$c_H = 10.533$ (1) Å	$V_H = 841.3$ (1) Å^3
	$a_H = 9.547$ (1) Å	$c_H = 10.378$ (1) Å	$V_H = 819.3$ (1) Å^3
Unit cell refined from 25 reflections ($9° < \theta < 15°$)			Z: 1
$\rho_{cal} = 7.22, 6.97, 7.72, 6.53, 6.39$ g/cm^3			
Crystal size:			$0.093 \times 0.093 \times 0.07$ mm^3
			$0.14 \times 0.08 \times 0.07$ mm^3
			$0.12 \times 0.12 \times 0.12$ mm^3
			$0.16 \times 0.09 \times 0.07$ mm^3
			$0.046 \times 0.058 \times 0.07$ mm^3
Linear absorption factor: 32.5, 34.11, 35.02, 35.31, 17.56 mm^{-1}			

II. Data Collections

Temperature: 295 K	Wavelength: MoK_α radiation
Diffractometer: Enraf–Nonius CAD-4	Scan mode: $\omega - 2\theta$
Monochromator: graphite	Scan width: $1.20 + 0.35$ tg θ
$0 < h < 10$; $0 < k < 10$; $-10 < l < 10$	θ_{max}: 35
Number of measured reflections 1021, 989, 914, 719, 929	
Number of independent reflections (with $I > \sigma(I)$): 788, 737, 795, 765, 815	

III. Structure Determination

Lorentz and polarization corrections
Absorption Correction: DIFABS, PSISCAN, SAC, PSISCAN, PSISCAN
Refinement on F
Refined parameters: 33, 45, 45, 45, 45
Number of independent reflections with $I > 3\sigma(I) = 726, 672, 765, 719, 651$
Unweighted agreement factor $R = 0.032, 0.029, 0.036, 0.029, 0.023$
Weighted agreement factor $R_\omega = 0.050, 0.036, 0.054, 0.044, 0.029$
Validity of refinement $S = 1.127, 1.026, 1.699, 1.07, 1.515$
Ponderation factor P: 0.07, 0.05, 0.05, 0.07, 0.04 $\omega = 4F_o^2/[\sigma^2(F_o^2) + (PF_o^2)^2]$
$\Delta\rho$ max: 2.11, 1.56, 2.16, 1.92, 1.07 e^- Å^3
$\Delta\rho$ min: -0.868, -0.549, -0.976, -0.522, -0.477 e^- Å^3
$(\Delta/\sigma)_{max} < 0.03, 0.02, 0.02, 0.01, 0.01$
Secondary Extinction coefficient: 6.788×10^{-7}, 1.87×10^{-7}, 2.312×10^{-6}, 2.55×10^{-6}, 1.706×10^{-6}
Atomic scattering factors from *International Tables of X-Ray Crystallography RX*

four different nominal stoichiometry: $Ni_yMo_6Se_8$, $Ni_yMoSe_6S_2$, $Ni_yMo_6Se_4S_4$, and $Ni_yMo_6Se_2S_6$.

X-ray diffraction intensities were collected on a Nonius CAD-4 four circle diffractometer with the experimental conditions given in Table 1. All the single crystals have the space group ($R\bar{3}$). All calculations were performed using the MOLEN program system (12). The results from the crystalline determinations are summarized in Tables 2 and 3.

TABLE 2
Positional Occupancy Factors and Thermal Parameters of $Ni_2Mo_6S_8$, $Ni_{1.99}Mo_6Se_{2.17}S_{5.83}$, $Ni_{1.85}Mo_6Se_{3.46}S_{4.54}$, $Ni_{1.82}Mo_6Se_{4.11}S_{3.89}$, $Ni_{1.28}Mo_6Se_{5.72}S_{2.28}$, and $Ni_{1.25}Mo_6Se_8$ ($B_{eq} = 4/3 \sum\sum a_i \cdot a_j B_{ij}$)

Atom	Site	x	y	z	B(Å^2)
		$Ni_2Mo_6S_8$ (14)			
Mo	6f	0.21743 (6)	0.40455 (6)	0.54305 (4)	0.58 (1)
S(1)	6f	0.3781 (2)	0.1330 (2)	0.7269 (2)	0.83 (1)
S(2)	2c	0.1999 (2)	0.1999 (2)	0.1999 (2)	0.81 (1)
Ni(1)	6f	0.0558 (11)	0.0791 (11)	0.8192 (10)	1.89 (8)
$\tau = 0.166$ (2)					
Ni(2)	6f	0.0144 (9)	0.3458 (9)	0.9404 (9)	1.45 (7)
$\tau = 0.166$(2)					
		$Ni_{1.99}Mo_6Se_{2.17}S_{5.83}$			
Mo	6f	0.21889 (4)	0.40569 (4)	0.54448 (4)	0.552 (4)
X(1)	6f	0.3768 (1)	0.1309 (1)	0.7303 (1)	0.91 (1)
0.20 Se/0.80S					
X(2)	2c	0.19420 (8)	0.19420 (8)	0.19420 (8)	1.067 (3)
0.49 Se/0.51S					
Ni(1)	6f	0.0588 (6)	0.0718 (7)	0.7920 (7)	2.48 (7)
$\tau = 0.152$(2)					
Ni(2)	6f	0.0048 (4)	0.3470 (5)	0.9366 (4)	1.31 (5)
$\tau = 0.179$(2)					
		$Ni_{1.85}Mo_6Se_{3.46}S_{4.54}$			
Mo	6f	0.22096 (5)	0.40749 (5)	0.54468 (5)	0.873 (4)
X(1)	6f	0.3749 (1)	0.1289 (1)	0.7346 (1)	1.167 (9)
0.32 Se/0.68S					
X(2)	2c	0.19697 (8)	0.19679 (8)	0.19679 (8)	1.275 (3)
0.77 Se/0.23S					
Ni(1)	6f	0.0620 (10)	0.0750 (10)	0.7870 (10)	3.0 (1)
$\tau = 0.105$ (2)					
Ni(2)	6f	−0.0004 (5)	0.3470 (6)	0.9368 (5)	2.10 (6)
$\tau = 0.203$ (2)					
		$Ni_{1.82}Mo_6Se_{4.11}S_{3.89}$			
Mo	6f	0.22173 (5)	0.40819 (5)	0.54477 (5)	0.440 (5)
X(1)	6f	0.3749 (1)	0.1283 (1)	0.7360 (1)	0.709 (9)
0.405 Se/0.595S					
X(2)	2c	0.19825 (8)	0.19825 (8)	0.19825 (8)	0.877 (3)
0.84 Se/0.16S					
Ni(1)	6f	0.061 (1)	0.075 (2)	0.787 (2)	3.6 (2)
$\tau = 0.098$ (3)					
Ni(2)	6f	0.0016 (6)	0.3468 (7)	0.9363 (7)	1.87 (7)
$\tau = 0.205$ (2)					
		$Ni_{1.28}Mo_6Se_{5.72}S_{2.28}$			
Mo	6f	0.22420 (5)	0.41165 (5)	0.54586 (5)	0.703 (5)
Se(1)	6f	0.37547 (9)	0.12661 (8)	0.73992 (9)	0.944 (8)
0.65 Se/0.35S					
Se(2)	2c	0.20498 (8)	0.20498 (8)	0.20498 (8)	1.073 (7)
0.91 Se/0.09S					
Ni(2)	6f	−0.0013 (9)	0.3440 (10)	0.9359 (8)	3.2 (1)
$\tau = 0.168$ (3)					
Ni(2′)	6f	0.508 (2)	0.956 (2)	0.846 (2)	0.6 (2)
$\tau = 0.045$ (2)					
		$Ni_{1.25}Mo_6Se_8$			
Mo	6f	0.22924 (7)	0.41922 (7)	0.54805 (7)	0.468 (7)
Se(1)	6f	0.37670 (9)	0.12382 (9)	0.74339 (9)	0.763 (9)
Se(2)	2c	0.21714 (9)	0.21714 (9)	0.21714 (9)	0.833 (4)
Ni(2′)	6f	0.5000 (6)	0.9436 (5)	0.8406 (5)	0.67 (5)
$\tau = 0.208$ (2)					

The chalcogen positions (Table 2) were first assumed to contain only Se (or S if in the majority) with fractional occupancy; then the positional and thermal parameters were fixed to the refined values, and the occupancies of the chalcogen positions by Se and S were refined, constrained to full occupancy of the eight available positions. Then Ni occupancy rates were refined. These occupancy rates, of course, vary with the chalcogen ratio.

We represent in Fig. 4 the evolution of the y_{max} cation content in each compound as a function of the x sulfur content. The pure selenide compound can only accept 1.25 Ni per unit cell against 2 in the pure sulfide one.

This curve exhibits a jump near $x = 4$.

For $x \leq 3$, the $Ni_yMo_6Se_{8-x}S_x$ pseudoternary seems to accept only 1.30 nickel cation and for $x \geq 4$ it is possible to insert between 1.80 and 2 nickel cations per Mo_6X_8 unit. This property was often noted that the selenium Chevrel phases contain less small cations content than the sulfur ones because of covalency of Se atoms.

The Chevrel phases structure which consists of a stacking of Mo_6X_8 quasi-cubic building blocks is represented on Fig. 5. This stacking leaves three types of cavity in the chalcogen lattice. The cavity 1 (the largest one) is a quasi-cubic shaped cavity located at the origin of the rhombohedral unit-cell with point symmetry $\bar{3}$; it is formed by eight chalcogen atoms belonging to eight different Mo_6X_8 units. The cavity 2, situated at the middle of the rhombohedral axes ($\bar{1}$ point symmetry), has more irregular cubic shape (X_8) and is formed by eight chalcogen atoms belonging to four different Mo_6X_8 units. This cavity 2 shares opposite pseudo-squared faces with two other cavities 1 along the rhombohedral axes. Cavity 3, formed by eight chalcogen atoms belonging to two different Mo_6X_8 units, is always empty because of the Mo–Mo intercluster bond going through.

We have followed the evolution of the location of the nickel cations in the whole solid solution, thanks to the refined cation position. The Ortep representations of occupancy of cavities 1 and 2 by nickel cations are shown on Fig. 6 (13). The occupancy rate of the sites (labeled 1 in cavity 1 and 2 or 2′ in cavity 2 of the Chevrel phases' structure) as a function of x, sulfur content, has been schematized in Fig. 7.

The $Ni_2Mo_6S_8$ structure (14) has been chosen as a reference to define the cavities and the positions where the atomic coordinates of nickel cations are located. We differentiate two types of positions in cavity 2 because of the atomic coordinates found for $Ni_{1.28}Mo_6Se_{5.72}S_{2.28}$ (see Tables 2 and 3). One type of positions in cavity 2 is very similar to the type met in the structure of $Ni_2Mo_6S_8$ (14). So we named them Ni(2). The other type of positions are nearly those found in the $Ni_{0.66}Mo_6Se_8$ (9) triclinic selenide compound, so they are called (Ni(2′)).

This new occupation of channels of $Ni_{1.28}Mo_6Se_{5.72}S_{2.28}$ by nickel ions is quite original and allows us to well understand the differences in site occupancy between the pure sulfide and the pure selenide.

So we are able to follow the evolution of the location of the nickel cations in the whole solid solution in the

TABLE 3
Principal Distances (Å) and Angles (°) of $Ni_{1.25}Mo_6Se_8$, $Ni_{1.28}Mo_6Se_{5.72}S_{2.28}$, $Ni_{1.82}Mo_6Se_{4.11}S_{3.89}$, $Ni_{1.85}Mo_6Se_{3.46}S_{4.54}$, $Ni_{1.99}Mo_6Se_{2.17}S_{5.83}$, and $Ni_2Mo_6S_8$

Distances (Å)	$Ni_{1.25}Mo_6X_8$ $X_8=Se_8$	$Ni_{1.28}Mo_6X_8$ $X_8=Se_{5.72}S_{2.28}$	Distances (Å)	$Ni_{1.82}Mo_6X_8$ $X_8=Se_{4.11}S_{3.89}$	$Ni_{1.85}Mo_6X_8$ $X_8=Se_{3.46}S_{4.54}$	$Ni_{1.99}Mo_6X_8$ $X_8=Se_{2.17}S_{5.83}$	$Ni_2Mo_6S_8$ (14)
Mo_6X_8 cluster unit			Mo_6X_8 cluster unit				
Intratriangle	2.686	2.694	Intratriangle				
(Mo–Mo)Δ			(Mo–Mo)Δ	2.700	2.703	2.702	2.691
Intertriangle	2.760	2.778	Intertriangle				
MoΔ–MoΔ			MoΔ–MoΔ	2.777	2.775	2.770	2.765
Intercluster Mo–Mo	3.355	3.293	Intercluster Mo–Mo	3.265	3.254	3.217	3.185
Mo–$X(2)$	2.571	2.573	Mo–$X(2)$	2.574	2.573	2.559	2.477
$X(1)$	2.562	2.518	$X(1)$	2.448	2.476	2.437	2.408
$X(1)$	2.608	2.562	$X(1)$	2.526	2.514	2.477	2.451
$X(1)$	2.623	2.603	$X(1)$	2.587	2.577	2.534	2.496
Intercluster Mo–$X(1)$	2.655	2.575	Intercluster Mo–$X(1)$	2.534	2.522	2.484	2.460
$X(2)$–$X(1)$	3.747	3.746	$X(2)$–$X(1)$	3.717	3.706	3.663	3.577
$X(1)$–$X(1)$	3.576	3.507	$X(1)$–$X(1)$	3.468	3.454	3.400	3.353
X_8 origin (org) cubic site			X_8 origin cubic site				
$X(2)$–$X(1)$	3.443	3.366	$X(2)$–$X(1)$	3.342	3.329	3.336	3.360
$X(1)$–$X(1)$	3.587	3.546	$X(1)$–$X(1)$	3.528	3.525	3.524	3.523
org(1)–$X(2)$	2.450	2.223	org(1)–$X(2)$	2.101	2.073	2.015	2.047
org(1)–$X(1)$	3.216	3.205	org(1)–$X(1)$	3.210	3.213	3.223	3.229
$X(1)$–$X(2)$–$X(1)$ angle(°)	101.70	105.03	$X(1)$–$X(2)$–$X(1)$ angle(°)	106.75	107.13	107.98	107.32
Site 2′/cavity 2			Site 1/cavity 1				
Ni(2′)–Ni(2′)	2.253	2.106	Ni(1)–Ni(1)	1.655	1.653	1.601	1.403
				2.706	2.706	2.613	2.370
Ni(2′)–$X(2)$	2.258	2.263		3.172	3.171	3.064	2.755
$X(1)$	2.188	2.115	Ni(1)–$X(2)$	2.405	2.385	2.308	2.335
$X(1)$	2.243	2.171	$X(1)$	2.110	2.116	2.149	2.220
$X(1)$	2.517	2.574	$X(1)$	2.121	2.117	2.155	2.220
Ni(2′)–Ni(2)	—	1.309	$X(1)$	2.841	2.817	2.736	2.592
Site 2/cavity 2			Site 2/cavity 2				
Ni(2)–Ni(2)	—	2.196	Ni(2)–Ni(2)	2.132	2.119	2.104	2.105
	—	2.919		2.923	2.909	2.896	2.902
Ni(2)–$X(2)$	—	2.440	Ni(2)–$X(2)$	2.386	2.380	2.333	2.292
$X(1)$	—	2.199	$X(1)$	2.184	2.172	2.167	2.194
$X(1)$	—	2.214	$X(1)$	2.234	2.230	2.278	2.330
$X(1)$	—	2.541	$X(1)$	2.508	2.515	2.481	2.446
			Ni(1)–Ni(2)	0.984	0.973	1.002	1.187
				2.059	2.060	2.026	1.879
				2.529	2.515	2.500	
			Ni(1)–Mo	2.975	2.965	2.974	3.040
Ni(2)–Mo		3.009		2.973	2.949	2.940	2.978
		3.099		3.076	3.079	3.034	3.014
		3.422		3.301	3.285	3.198	3.090
Ni(2′)–Mo	2.481	2.460					
	2.848	2.811					
	2.904	2.888					
			Org(1)–Ni(1)	1.586	1.585	1.532	1.378
			Org(2)–Ni(1)	1.926	1.917	1.924	
				3.109	3.100	3.068	
Org(2)–Ni(2)	—	1.098	Org(2)–Ni(2)	1.066	1.059	1.052	1.052
Org(1)–Ni(2)	—	2.342	Org(1)–Ni(2)	2.347	2.344	2.325	2.300
Org(2)–Ni(2′)	1.127	1.053					
Org(1)–Ni(2′)	3.505	3.357					
Org(2)–Mo	3.175	3.029	Org(2)–Mo	2.955	2.936	2.886	
	3.490	3.466			3.447		

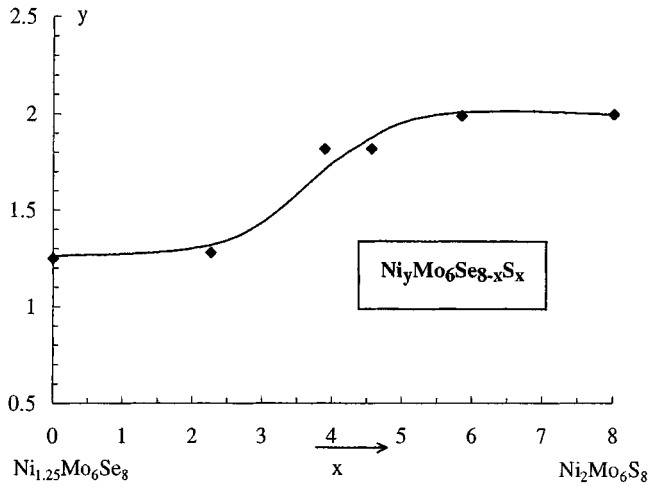

FIG. 4. Evolution of the nickel maximum content y_{max} versus the x sulfur content of $Ni_yMo_6Se_{8-x}S_x$.

chalcogen network while sulfur atoms substitute for selenium atoms.

In $Ni_{1.25}Mo_6Se_8$, the nickel ions are only in one six-fold position in cavity 2 (site 2′: Ni(2′) cations). The occupancy is $\tau(Ni(2')) = 0.208$ and the nickel ions are in a tetrahedral coordination of selenium atoms (distances Ni(2′)–Se(2), 2.258 Å, and Ni(2′)–Se(1), 2.188, 2.243, and 2.517 Å).

In $Ni_{1.28}Mo_6Se_{5.73}S_{2.27}$, the nickel ions can occupy two six-fold positions in the same cavity 2. The Ni(2′) ions (site 2′) are in tetrahedral sites of chalcogen atoms as the nickel atoms in the previous structure. The occupancy of this site 2′ decreases ($\tau = 0.045$) with respect to one of the pure selenide. The Ni(2) ions occupy the site 2 so in the cavity 2 (occupancy of 0.168) and are in tetrahedral environment of chalcogen atoms, this tetrahedron sharing one face with the precedent tetrahedron. But it looks evident that these tetrahedra are not filled in the same cell, because the distance Ni(2′)–Ni(2) = 1.309 Å is really too short. The distances Ni(2)–Ni(2), 2.199 Å, and Ni(2′)–Ni(2′), 2.106 Å (via $\bar{1}$), are also very short to have metal–metal bondings. The drawing of Fig. 6 allows one to understand why the equivalent thermal parameter of Ni(2′) is smaller than that of Ni(2): it is because the Ni(2′) site is much smaller than the Ni(2) site (see the Ni–Se distances).

Thus, the following structure of nickel molybdenum sulfoselenides is very close to the $Ni_2Mo_6S_8$ structure. The nickel ions occupy equivalent positions in the cavity 2 (Ni(2) atoms) and in the cavity 1 (Ni(1) atoms) for the three new structures; only the occupancy factors change, being

$\tau(Ni(2)) = 0.205(2)$ $\tau(Ni(1)) = 0.098(3)$
$\tau(Ni(2)) = 0.203(2)$ $\tau(Ni(1)) = 0.105(2)$
$\tau(Ni(2)) = 0.179(2)$ $\tau(Ni(1)) = 0.152(2)$
$\tau(Ni(2)) = 1/6\ (0.167)$ $\tau(Ni(1)) = 1/6\ (0.167)$

in $Ni_{1.82}Mo_6Se_{4.11}S_{3.89}$, $Ni_{1.85}Mo_6Se_{3.46}S_{4.54}$, $Ni_{1.99}Mo_6Se_{2.17}S_{5.83}$, and $Ni_2Mo_6S_8$, respectively.

The schema of occupancy evolution (Fig. 7) shows that site 2′ empties quickly while site 2 fills when sulfur atoms start to substitute for selenium atoms in these phases. Note that we have not checked if a compound can exist containing Ni cations in the three sites at the same time for $x \sim 3$. The possibility of nickel cations occupying very roughly

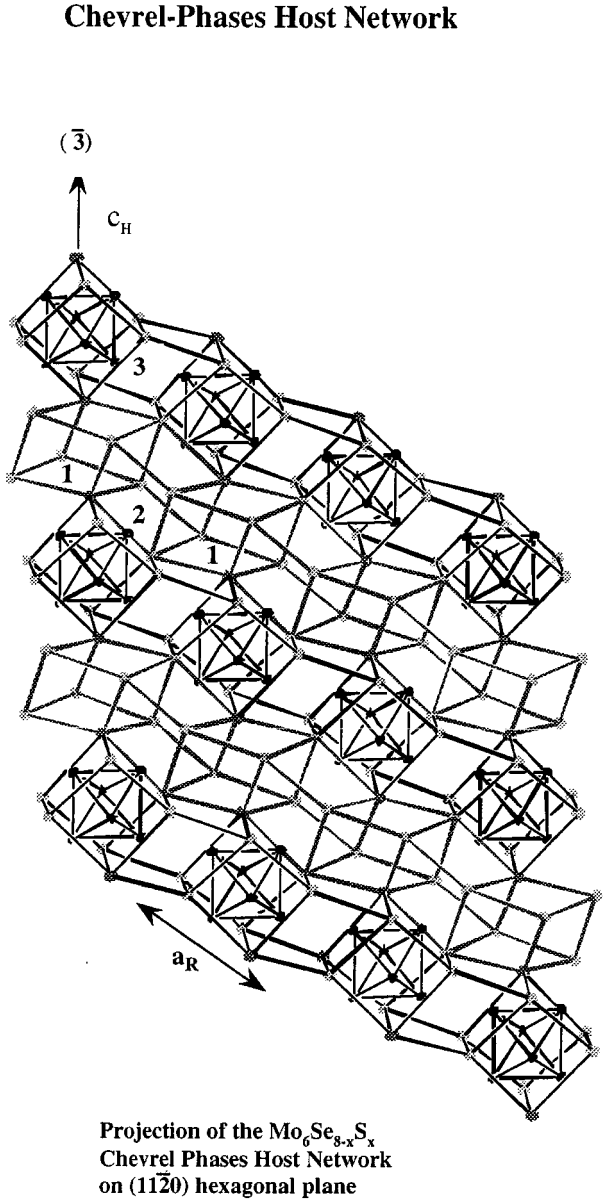

FIG. 5. Projection of the host network $Mo_6Se_{8-x}S_x$ on hexagonal plane of $Ni_yMo_6Se_{8-x}S_x$ compounds. View of the chalcogen channels with the three types of cavities.

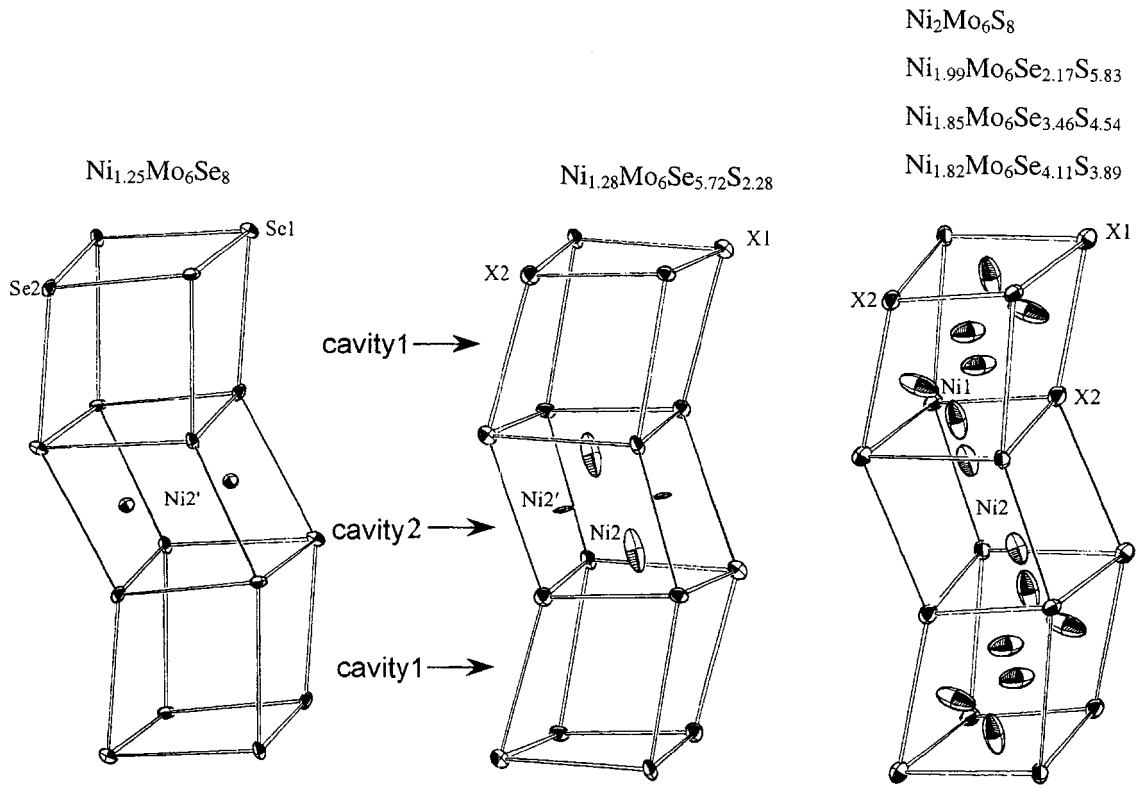

FIG. 6. Location of the nickel ions in cavities 1 and 2 of the host network of the different $Ni_yMo_6Se_{8-x}S_x$ single crystals along the x chalcogen solid solution.

site 1 instead of the site 2′ ($x \sim 3$–4) can probably explain the jump of y_{max} exhibited in Fig. 4, the sulfoselenide compound can now accept much more Ni cations in the host network.

Near $x = 2.5$–3, site 1 begins to be occupied and only for $Ni_2Mo_6S_8$, the occupancies of sites 1 and 2 are equal (14). In view of all these results, we conclude that the jump found in the representation of the α_R parameter as a function of x for $Ni_{1.2}Mo_6Se_{8-x}S_x$ or of y_{max} versus x in $Ni_{y_{max}}Mo_6Se_{8-x}S_x$ single crystals is due to massive occupancy of site 1.

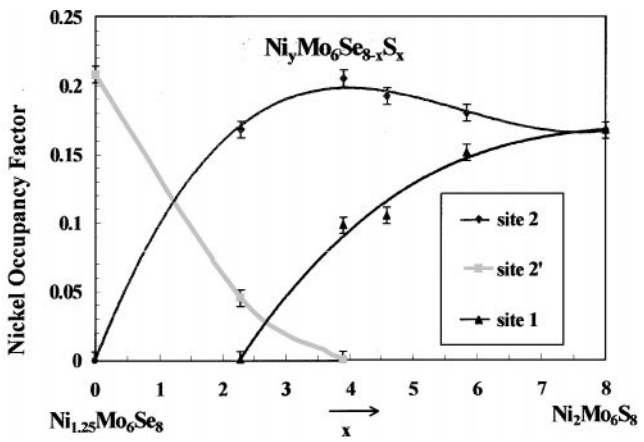

FIG. 7. Nickel occupancy factors in the three different sites of the $Ni_yMo_6Se_{8-x}S_x$ solid solution.

These structural investigations give also precious information on the chalcogen arrangement. The refined chalcogen occupancies are reported in Table 2. There is no real ordering S/Se in the solid solution, but the disorder is not perfect; actually the selenium atoms occupy the special 2c position preferentially.

Tarascon and co-workers predicted no ordering for the mixed Chevrel phases, except for $LaMo_6Se_{8-x}S_x$ (5), but their considerations were only based on the variation of c_H/a_H determined from X-ray powder diagrams versus the chalcogen ratio. Our conclusions are a little bit different, since it is clear that selenium atoms take one preferential place in special 2c positions for Chevrel phases with small cations, and in general 6f positions with large cations, whatever the chalcogen ratio.

The copper mixed solid solution seems to exhibit the same feature if we consider the two single structure determinations for $Cu_{2.6}Mo_6Se_{6.5}S_{1.5}$ and $Cu_{2.6}Mo_6Se_{3.4}S_{4.6}$ reported by McKinnon and co-workers (6, 7). But there is a main difference between the nickel and copper solid solutions: for the 6Se/2S composition, the copper cations are actually statistically localized in cavity 1, site 1 and in

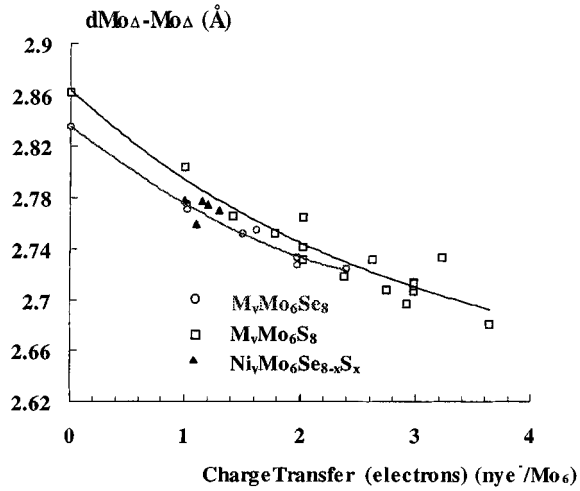

FIG. 8. Variation of the Mo_Δ–Mo_Δ intertriangle distance as function of electronic charge transfer in $M_yMo_6S_8$, $M_yMo_6Se_8$, and $Ni_yMo_6Se_{8-x}S_x$ compounds from model of Yvon (16).

cavity 2, site 2 (τ(Cu(2)) $\sim$ τ(Cu(1)) $\sim$ 0.21) and we have seen for the corresponding nickel compound that nickel cations occupy two different sets of positions only in cavity 2 (Ni(2) and Ni(2′)) with different occupancies (τ(Ni(2)) = 0.170; τ(Ni(2′)) = 0.045).

In $Cu_{y_{max}}Mo_6Se_{8-x}S_x$, copper cation occupies statistically site 1 and site 2, even at $x = 8$ or $x = 0$ (6, 7) while in $Ni_{y_{max}}Mo_6Se_{8-x}S_x$, the occupancy of each site (sites 1, 2, 2′) depends on the Se/S ratio (Fig. 7).

So the nickel mixed Chevrel phases exhibit an interesting feature in the location of these cations in the chalcogen network, allowing the transition between the pure sulfide and selenide nickel Chevrel phases to be well understood.

In the $M_y^{n+}Mo_6X_8$ Chevrel phases, a charge transfer of $(n.y)e^-/Mo_6$ occurs through Mo_6 cluster and Mo_Δ–Mo_Δ intertriangle distances of the cluster (16). Yvon has reported for a large number of Chevrel phases the variation of the Mo_Δ–Mo_Δ intertriangle distances versus charge transfer and established the model of Fig. 8.

We report our data from $Ni_yMo_6Se_{8-x}S_x$. For these compounds, the electronic charge transfer from nickel atoms through the Mo_6 cluster seems to be quasi-constant, because there is no significant change in Mo_Δ–Mo_Δ distances, even if the nickel amount rises in richer sulfur compounds. The mean distance is around 2.77 Å, which indicates a charge transfer model with between 1 and $1.4e^-$/Mo according to the nature of chalcogen (Table 4). We deduced from this model the formal oxidation state of nickel cations; it is between 0.60 and 0.90. It is not a common oxidation state for nickel cation in solid state chemistry, which leads us to conclude that electrons exist near nickel cations.

TABLE 4
Charge Transfer and Oxidation State of Nickel Cation for $Ni_yMo_6Se_{8-x}S_x$ from Model of Yvon (16)

Compounds	Charge transfer $(ny)e^-/Mo_6$	Charge of cation n^+
$Ni_{1.25}Mo_6Se_8$	1.1	0.88
$Ni_{1.25}Mo_6Se_{5.72}S_{2.28}$	1	0.78
$Ni_{1.82}Mo_6Se_{4.11}S_{3.89}$	1.15	0.63
$Ni_{1.85}Mo_6Se_{3.46}S_{4.54}$	1.2	0.65
$Ni_{1.99}Mo_6Se_{2.17}S_{5.83}$	1.3	0.65
$Ni_2Mo_6Se_8$	1.4	0.7

We suspect that Ni–Ni bondings shape cationic clusters $(Ni_2)^{2+}$, $(Ni_3)^{2+}$ … because magnetic susceptibility measurements made on $Ni_{1.82}Mo_6Se_{4.11}S_{3.89}$ indicated only Pauli paramagnetism (No Curie/Weiss-type magnetism, typical for Ni^{2+} in tetrahedral sites, can be detected.) Moreover, Schöllhorn proposed earlier polynuclear models for $(Zn_2)^{2+}Mo_6S_8^{2-}$, $(Cd_2)^{2+}Mo_6S_8^{2-}$, and $(Li_4)^{3+}Mo_6S_8^{3-}$, and suspected them to be available for Co, Fe, and Ni in Chevrel phases (17, 18). Note that nickel clusters are compatible with the cationic sites geometry. In site 1, the six equivalent positions (6f) form a hexagon and we can easily imagine as occupied one over two positions forming $(Ni_3)^{2+}$ triangular complex. In the same way, in site 2, we can have $(Ni_2)^{2+}$ pairs from a geometric point of view. These assumptions are reinforced by the high mobility of the nickel atoms in nickel molybdenum sulfide (19).

In the pure nickel Chevrel selenide and the mixed close selenide $Ni_{1.28}Mo_6Se_{5.72}S_{2.28}$, the nickel atoms are delocalized in cavity 2 (site 2 and site 2′), interact strongly with the Molybdenum atoms of the Mo_6 octahedral cluster, and can form Ni–Mo bondings (Table 3).

IV. CONCLUSION

We showed that $Ni_{y_{max}}Mo_6Se_{8-x}S_x$ solid solution containing the richest phases in nickel cations crystallizes in rhombohedral symmetry. The nickel amount varies from 1.25Ni/Mo_6 in the case of the selenide compound to 2Ni/Mo_6 in the case of the sulfide.

For substitution of smaller sulfur atoms for selenium ones, the nickel amount increases graduated in these phases where only the cavity 2 is occupied. Thus, the greater increase in the nickel amount is made possible when the rate of substitution is close to 3–4S, because the nickel cations can then fill cavity 1 of the host network.

This study permits us to understand the filling of the cavities of the sulfoselenide host network by nickel cations and to follow the structural evolution from $Ni_2Mo_6S_8$ to $Ni_{1.25}Mo_6Se_8$.

We also show that the nickel cations cannot be in the $+2$ oxidation state. They can form nickel clusters inside cavities of these phases or form bondings with Mo atoms belonging to the Mo_6 cluster.

REFERENCES

1. B. T. Matthias, M. Marezio, E. Corenzwit, A. S. Cooper, and H. F. Barz, *Science* **175,** 1465 (1972).
2. Ø. Fischer, H. Jones, G. Bongi, M. Sergent, and R. Chevrel, *J. Phys. C* **7,** L450 (1974).
3. T. Caillat, J.-P. Fleurial, and G. J. Snyder, *Solid State Sci.* **1**(7–8), 535 (1999); C. Roche, P. Pecheur, G. Toussaint, A. Jenny, H. Scherrer, and S. Scherrer, *J. Phys. Condens. Matter* **10,** L333 (1998); C. Roche, R. Chevrel, A. Jenny, P. Pecheur, H. Scherrer, and S. Scherrer, *Phys. Rev. B* **60,** 16,442 (1999).
4. R. Chevrel, M. Sergent, and Ø. Fischer, *Mater. Res. Bull.* **10,** 1169 (1975).
5. D. C. Johnson, J. M. Tarascon, and M. J. Sienko, *Inorg. Chem.* **22,** 3773 (1983).
6. L. S. Selwyn, W. R. McKinnon, J. R. Dahn, and Y. Le Page, *Phys. Rev. B* **33,** 6405 (1986).
7. L. S. Shenoy, W. R. McKinnon, and Y. Le Page, *Phys. Rev. B* **42,** 10,427 (1990).
8. M. Sergent and R. Chevrel, *C. R. Acad. Sci.* **274,** 1965 (1972); *J. Solid State Chem.* **6,** 433 (1973).
9. O. Bars, J. Guillevic, and D. Grandjean, *J. Solid State Chem.* **6,** 335 (1973).
10. W. Honle and K. Yvon, *J. Solid State Chem.* **70,** 235 (1987).
11. R. Chevrel and M. Sergent, *in* "Superconductivity in Ternary Compounds, I" (Ø. Fischer and M. B. Maple, Eds.), Topics of Current Physics, Vol. 32, pp. 25–86. Springer-Verlag, Berlin/Heidelberg, 1982.
12. C. K. Fair, "MOLEN. An Interactive Intelligent System for Crystal Structure Analysis." Enraf-Nonius, Delft, 1990.
13. C. K. Johnson, "ORTEP II," Report ORNL-5138, Oak Ridge National Laboratory, 1976.
14. J. Guillevic, O. Bars, and D. Grandjean, *J. Solid State Chem.* **7,** 158 (1973); *Acta Crystallogr. Sec. B* **32,** 1338 (1976).
15. K. Yvon, R. Chevrel, and M. Sergent, *Acta Crystallogr. Sect. B* **36,** 685 (1980).
16. K. Yvon, *in* "Current Topics in Materials Science," (E. Kaldis, Ed.), Vol. 3, 53. North-Holland, Amsterdam, 1979.
17. R. Schöllhorn, "Inclusion Compounds," p. 249, Academic Press, London, 1984.
18. C. Prigge, W. Müller-Warmuth, E. Gocke, and R. Schöllhorn, *Solid State Ionics* **62,** 143 (1993).
19. C. Ritter, C. Nöldeke, W. Press, U. Stege, and R. Schollhorn, *Z. Phys. B* **92,** 437 (1993).